

HARDENABILITY STUDY OF LOW ALLOY SINTERED STEELS CONTAINING MANGANESE

M. Zendron, A. Molinari, L. Girardini

Abstract

The hardenability of three low alloy Mn steels was studied in a vacuum furnace on specimens with different cross sections quenched with different pressures of cooling nitrogen. The results are expressed in terms of microhardness and percentage of martensite as a function of the carbon content and of the actual cooling rate in the specimens. This approach makes the results independent of the process parameters and applicable to each industrial condition, once the actual cooling rate in the parts is known.

Keywords: manganese, hardenability, low alloy steels

INTRODUCTION

Despite the positive effect on mechanical strength, toughness and hardenability, the use of manganese as an alloying element for Powder Metallurgy steels is still limited. The main reason lies in the lack of confidence with its behaviour on sintering, in particular in industrial furnaces, but the search for new materials for the structural applications of sintered steels could lead to a progressive increment, even because it is less expensive than other alloying elements, such as Ni and Mo. The sintering behaviour of Mn steels has been extensively studied by several authors [1-9], and its effect on dimensional variations, microstructure and mechanical properties is well documented. As said before, Mn increases hardenability of steels as well, and therefore it is expected to have a great potential in through hardening, carburizing and sinterhardening [10,11].

In the present work the hardenability of three new prealloyed powders containing manganese has been investigated, under the typical conditions of vacuum furnaces with gas cooling, and of sinterhardening in atmosphere furnaces [12]. Reference has been made to the actual cooling rate in the specimens in order to get results which are independent of the cross section of pieces and on the cooling conditions, and which directly indicate the capability of austenite to transform into martensite on cooling. Powders were mixed with different amounts of graphite, in order to cover a wide range of carbon concentrations. Hardenability was evaluated by microhardness, and reference was made to a minimum martensite content of 50% [13]. The microstructural analysis was carried out as well, and the volumetric fraction of martensite was measured by means of Image Analysis.

The aim of this work is to determine the minimum cooling rate which has to be guaranteed in the parts to produce a hardened microstructure, in dependence on the carbon content.

EXPERIMENTAL PROCEDURE

The nominal composition of the prealloyed powders used in the present work is reported in Table 1.

Tab.1. Nominal composition (wt.%) of the powders.

powder	% Mn	% Cr	% Ni	% Mo
E	0.8	1	-	-
F	1.2	0.2	-	-
G	0.7	1.2	0.4	0.4

The reaction occurring during sintering between graphite and the oxygen contained in the powder particles [14,15] results in some decarburization (about 0.12-0.15% carbon loss). A corresponding extra amount of graphite was then added to obtain the sintered carbon contents of 0.30%, 0.50% and 0.80%, which were confirmed by LECO CS244 analyses. Two types of specimens were produced for hardenability tests: disks 5 mm in diameter and of 10 mm height and Charpy impact bars of 10x10x55 mm. Disks 25 mm in diameter and 25 mm height were also produced, to determine the correlation between the cross section and the actual cooling rate over a wide range of diameters. Specimens were cold compacted to 6.8 g/cm³ and sintered in a 90N₂/10H₂ atmosphere at 1250°C, 30 minutes. Heat treatment was carried out in a TAV Minijet HP vacuum furnace. By means of ThermoCalc [16] the phase diagrams of the materials were calculated: they are shown in Figs.1, 2 and 3.

The austenitization temperature was set up at $A_3(A_{cm})+20^\circ\text{C}$ and the isothermal holding time was 30 minutes. The cooling rate was varied by changing the pressure of the cooling nitrogen, and the actual cooling rate was recorded by means of a thermocouple inserted in the central axis of the specimens. The combination of three nitrogen pressures, 2, 5 and 8 bars, with the two cross sections of the specimens resulted in the cooling rates reported in Table 2; they range between 4.6 K/s (impact bars quenched with the lowest pressure) and 31.5 K/s (5 mm diameter cylinders quenched with the highest pressure).

Tab.2. Cooling rate as a function of dimension and nitrogen pressure.

Dimension [mm]	N ₂ Pressure [bar]	Cooling rate [K/s]
25	2	2.2
	5	4.6
	8	6.1
10	2	4.6
	5	8.2
	8	10.6
5	2	16.9
	5	26
	8	31.5

Since the minimum cooling rate exceeds that of industrial sinterhardening processes in atmosphere furnaces, some materials were heat treated with a cooling nitrogen pressure of 1.5 bar using four impact bars bond together. This resulted in an actual cooling rate in the centre of the 20x20 mm cross section ranging between 1.8 and 2.9 K/s.

The microstructural analysis was carried out at the Light Optical Microscope on etched (50% Nital – 50% Picral) metallographic sections. By means of Image Analysis, the volumetric fraction of the martensite was measured. The HV0.1 microhardness was measured on the centre of the median cross section, by carrying out 15 measurements on each specimen. Data reported in the following is the mean value of the experimental results, excluding the lowest and the highest microhardness measured.

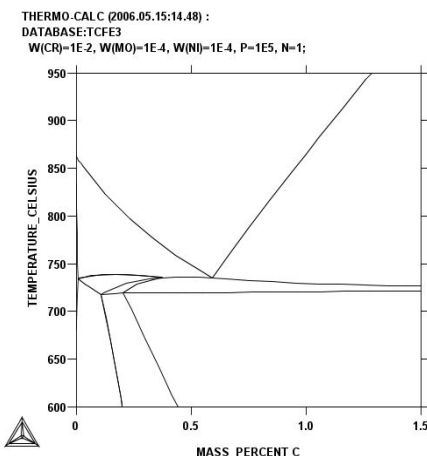


Fig.1. Phase diagram of material E.

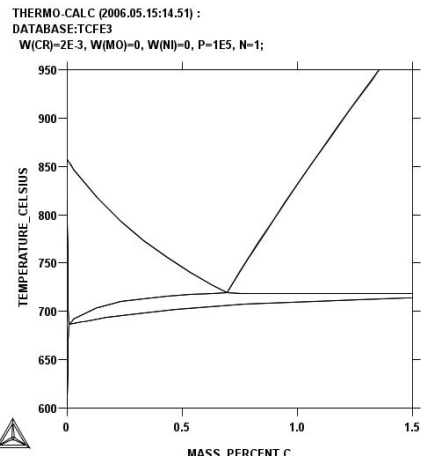


Fig.2. Phase diagram of material F.

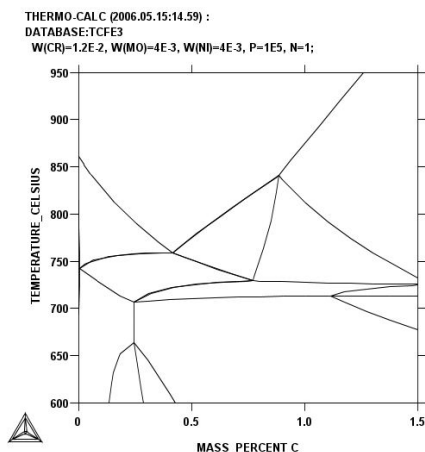


Fig.3. Phase diagram of material G.

RESULTS AND DISCUSSION

Figures 4, 5 and 6 report the microhardness vs. the sintered carbon content at the different cooling rates for materials based on powder E, F and G, respectively. As expected, the increase in the carbon content and in the cooling rate increases microhardness.

To evaluate hardenability, reference was made to the microhardness pertaining to a 50% martensite microstructure, for a given carbon content [ASTM A 255 – 02]. Hardening provided by the other alloying elements (all substitutional) was neglected, being less than that due to the interstitial carbon. Figures 7, 8 and 9 show microhardness vs. the cooling rate for the three carbon contents for materials based on powder E, F and G, respectively. In each graph, three horizontal lines are drawn as a reference, corresponding to the microhardness of a 50% martensite microstructure with 0.3% C, 0.5% C and 0.8% C. For a given carbon content, the experimental points lying above the reference line represent a condition of hardenability.

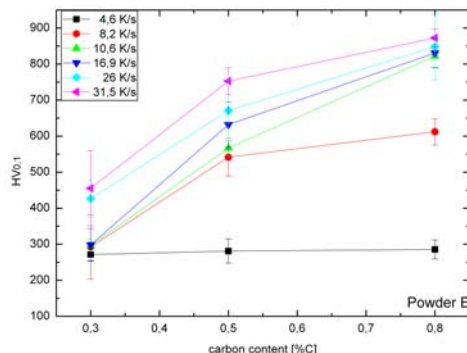


Fig.4. Correlation between microhardness, carbon content and cooling rate for the heat treated material E.

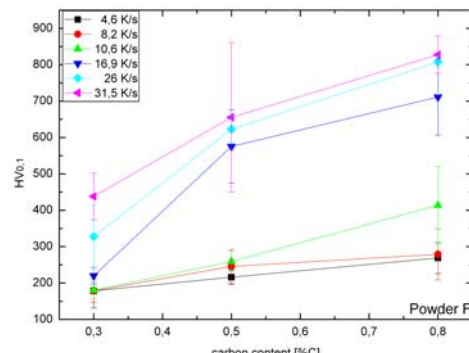


Fig.5. Correlation between microhardness, carbon content and cooling rate for the heat treated material F.

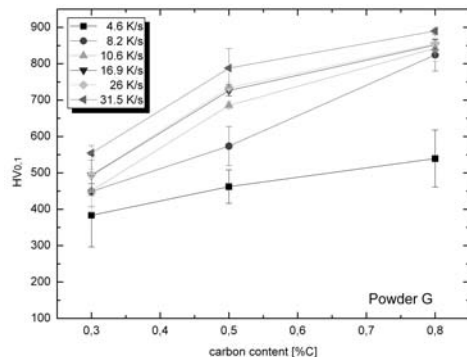


Fig.6. Correlation between microhardness, carbon content and cooling rate for the heat treated material G.

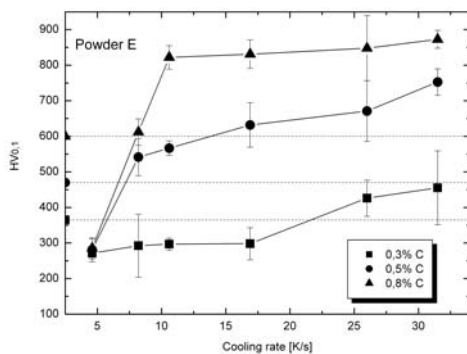


Fig.7. Minimum microhardness for hardened material E.

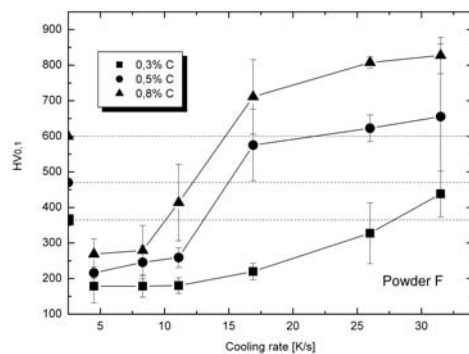


Fig.8. Minimum microhardness for hardened material F.

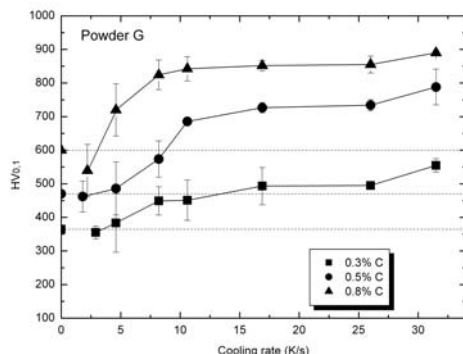


Fig.9. Minimum microhardness for hardened material G.

From the figures, the minimum cooling rate to obtain a hardened microstructure (under the assumption of 50% of martensite) for each carbon content can be determined. In particular:

- materials based on powder E: with 0.5% C and 0.8% C, they can be hardened with a cooling rate over about 8 K/s, whilst with the lowest carbon content, a minimum cooling rate of about 22 K/s has to be applied;
- materials based on powder F: with 0.5% C and 0.8% C, they can be hardened with a cooling rate over about 15 K/s, whilst with the lowest carbon content, a minimum cooling rate of about 27 K/s has to be applied;
- materials based on powder G: they can be hardened with a cooling rate over 4.6 K/s for all the carbon contents investigated.

Given their better response to heat treatment, the last materials were also quenched with a lower cooling rate. Figure 9 shows that they can be successfully hardened even with a cooling rate of about 2.5 K/s.

The microstructural analysis was carried out on all the specimens. On increasing carbon content and cooling rate, microstructures evolve:

- from a mixture of ferrite and pearlite to a full martensite in materials based on powder E (Figs.10 and 11);
- from a mixture of ferrite and pearlite to a mixture of lower bainite and martensite in materials based on powder F (Figs.12 and 13);
- from a mixture of upper bainite and martensite to a full martensite in materials based on powder G (Figs.14 and 15).

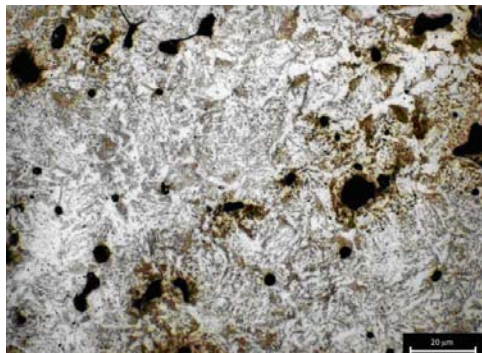


Fig.10. Powder E 0.3% C 4.6K/s – mixture of ferrite and pearlite.

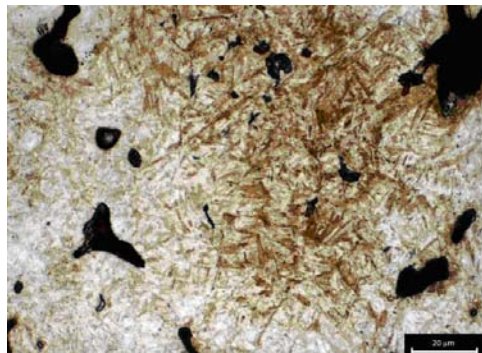


Fig.11. Powder E 0.8% C 31.5K/s – fully martensite.

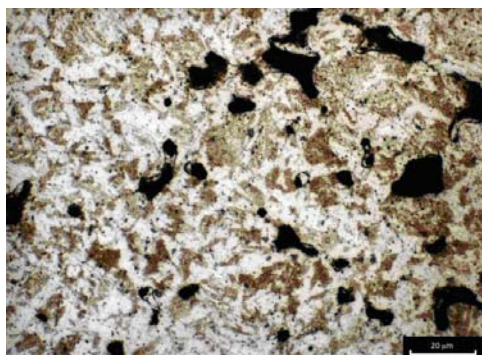


Fig.12. Powder F 0.3% C 4.6K/s – mixture of ferrite and pearlite.

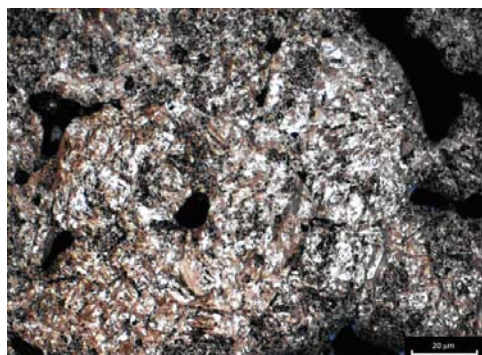


Fig.13. Powder F 0.8% C 31.5K/s – lower bainite and martensite.

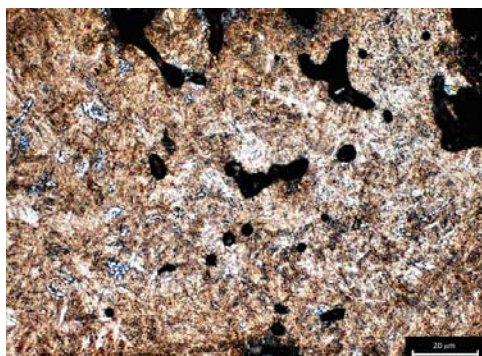


Fig.14. Powder G 0.3% C 4.6K/s – upper bainite and martensite.

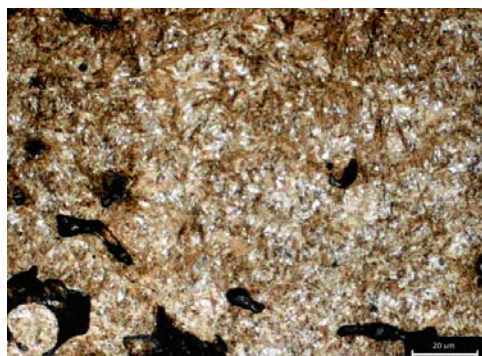


Fig.15. Powder G 0.8% C 31.5K/s – fully martensite.

The results of the quantitative evaluation of the volumetric percentage of martensite are reported in Tables 3, 4 and 5.

Tab.3. Volume percentage of martensite.

Powder E	% C		
K/s	0.3	0.5	0.8
4.6	0	37	42.7
8.2	0	79.4	89.1
10.6	0	87.6	100
16.9	41.3	100	100
26	60.9	100	100
31.5	63.2	100	100

Tab.4. Volume percentage of martensite.

Powder F	% C		
K/s	0.3	0.5	0.8
4.6	0	0	8.1
8.2	0	33.5	34.8
10.6	0	41.6	47.8
16.9	9.6	58.6	78
26	52.5	78.9	85.2
31.5	53.3	84.1	87.4

Tab.5. Volume percentage of martensite (n.a. = not available).

Powder G	% C		
K/s	0.3	0.5	0.8
1.8	n.a.	35.5	n.a.
2.2	n.a.	n.a.	50
2.9	47.1	n.a.	n.a.
4.6	70.8	80.9	86.4
8.2	75.9	87.2	100
10.6	80	88.6	100
16.9	84.2	100	100
26	100	100	100
31.5	100	100	100

The results confirm deductions from microhardness, since all the materials supposed to contain more than 50% of martensite, really do have such a microstructure.

The results of the quantitative analyses have been then elaborated, to obtain the microstructural maps reported in Figs.16, 17 and 18. Here, the “cooling rate – carbon content” space is subdivided in some areas, corresponding to different martensite percentages. In particular, the line corresponding to 50% of martensite defines the minimum actual cooling rate to harden the three materials, as a function of the sintered carbon content.

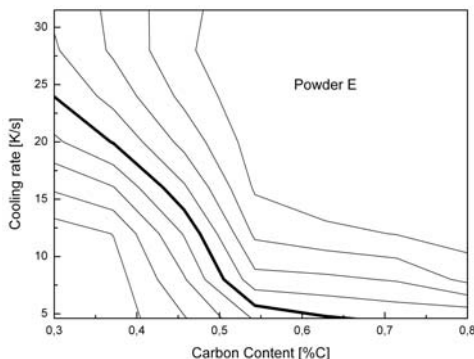


Fig.16. Hardenability map for the material E.

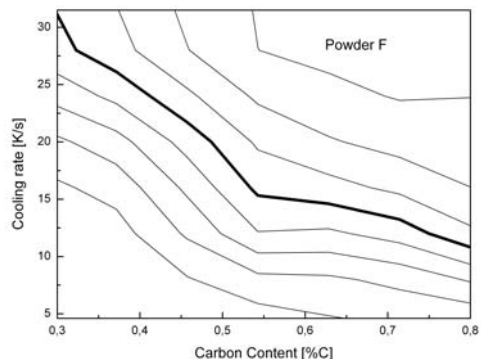


Fig.17. Hardenability map for the material F.

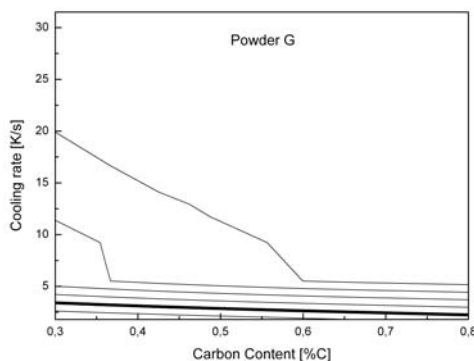


Fig.18. Hardenability map for the material G.

On the basis of the microhardness data and of the microstructural analysis, hardenability of the three materials at the same carbon content results $G > E > F$. Using the hardenability multiplying factors [13], the ideal diameters D_I of the three powders (at the same carbon content) result in the following ratios: $D_{I,G} = \sim 2.5 D_{I,E} = \sim 3 D_{I,F}$. Hardenability maps then confirm what can be deduced from ideal diameters. However the ideal diameters, which are frequently referred to for wrought steels, are not useful for sintered steels for two main reasons.

First, the Grossmann method is based on hardness, whilst in porous sintered steels microhardness is much more reliable in measuring the microstructural hardening, being not affected by porosity and by its possible heterogeneity in the real parts. Second, among the different hardening processes available in the technology of the wrought steels, each one qualified by a specific “severity of quench H”, only oil quenching is extensively applied in Powder Metallurgy. Vacuum quenching is used only for chromium steels, which have been introduced in industrial practice just over recent years. Sinterhardening is much more diffused in the PM industry, with cooling rates ranging between 2 and 4 K/s. Then, apart from oil and vacuum quenching, the typical cooling rates of the hardening processes of sintered steels are quite low, and they do not find a reliable reference in the Grossmann method.

Contrarily, the results of the present investigation may be used to design material for any specific application. In fact, from Figures 16, 17 and 18 it is possible to choose the

base powder and the carbon content to produce a hardened microstructure (50% martensite but, for specific cases, a fully martensitic microstructure), once the actual cooling rate in the pieces is known. The actual cooling rate depends on the cooling conditions and on the geometry and mass of pieces. In the case of the experiments presented here, Fig.19 shows this correlation for a density of 7.0 g/cm^3 , obtained by interpolating three sets of experimental determinations.

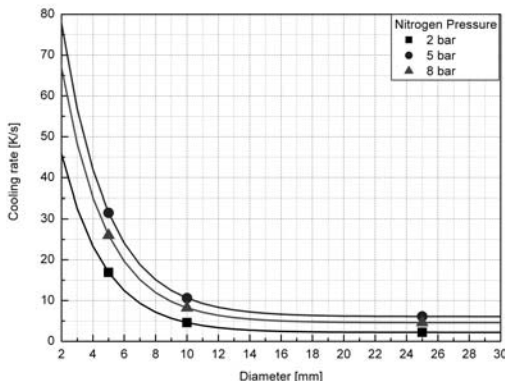


Fig.19. Correlation between dimension, nitrogen pressure and cooling rate.

CONCLUSIONS

The hardenability of different steels produced by using three low alloyed iron powders containing manganese has been studied by carrying out quenching experiments in a vacuum furnace with cooling in a pressurized nitrogen flow. The actual cooling rates, measured by a thermocouple in the central axis of the specimens, vary in the range 1.8–31.5 K/s. The results of the heat treatments were evaluated by means of microhardness, having the microhardness of the materials containing 50% of martensite for each carbon content as a reference. This microstructure represents the minimum condition to define steel as successfully hardened. Moreover, by means of a quantitative microstructural analysis, conclusions from microhardness have been confirmed, and the “hardenability maps” have been drawn. These maps give the minimum actual cooling rate to successfully harden the steels for various carbon contents. In addition, they provide helpful information to design the material and to select the pressure of cooling nitrogen for a specific requirement. Maps also give information on the “sinterhardenability” of the materials, since the range of cooling rate investigated covers those typical of the sinterhardening processes in the atmosphere furnaces.

In vacuum quenching, the actual cooling rate depends on the cross section of the specimens and on the pressure of the cooling nitrogen. By knowing this correlation, which has been experimentally determined, it is possible to correlate the minimum hardenable diameter with the carbon content and the nitrogen pressure.

Acknowledgements

This work has been carried out within the frame work of the Höganäs Chair project supported by Höganäs AB, Sweden.

REFERENCES

- [1] Šalak, A.: Powder Metall. Int., vol. 2, 1980, p. 72
- [2] Šalak, A., Dudrová, E., Miskovic, V.: Powder Metall. Sci. Technol., vol. 3, 1992, p. 26
- [3] Šalak, A., Selecká, M., Keresti, R., Parilák, L. In: Proceedings of Powder Metallurgy World Congress, Kyoto, 2000
- [4] Dudrová, E., Kabátová, M., Bidulský, R., Wronski, AS.: Powder Metallurgy, vol. 47, 2004, no. 2, p.181
- [5] Youseffi, M., Mitchell, SC., Wronski, AS., Cias, A.: Powder Metallurgy, vol. 43, 2000, no. 4, p. 353
- [6] Cias, A., Mitchell, SC., Watts, A., Wronski, AS.: Powder Metallurgy, vol. 42, 1999, no. 3, p. 277
- [7] Mitchell, SC., Becker, BS., Wronski, AS. In: Proceedings of Powder Metallurgy World Congress, Kyoto, 2000
- [8] Beiss, P. In: Proceedings of Advances in Powder Metallurgy & Particulate Materials, 2005
- [9] Campos, M., Sanchez, D., Torralba, JM.: Journal of Materials Processing Technology, vol. 143-144, 2003, p. 464
- [10] L'Espérance, G., Harton, S., deRege, A., Nigarura, S. In: Proceedings of Advances in Powder Metallurgy & Particulate Materials, 1995
- [11] Maroli, B., Berg, S., Larsson, M., Hauer, I. In: EUROMAT 2001. 7th European Conference on Advanced Materials and Processes, 2001, Italy
- [12] Stoyanova, V., Molinari, A.: Powder Metallurgy Progress, vol. 4, 2004, no. 2, p. 79
- [13] Reed-Hill, RE.: Physical Metallurgy Principles. PWS Publishing Company, 1994
- [14] Danninger, H., Gierl, C.: Materials Chemistry and Physics, vol. 67, 2001, p. 49
- [15] Danninger, H., Frauendienst, G., Streb, KD., Ratzi, R. : Materials Chemistry and Physics, vol 67, 2001, no. 1/3, p. 72
- [16] Sundman, B., Jansson, B., Andersson, JO.: Calphad, vol. 9, 1985, p. 153